China Instrument and Control Society
Instrumentation
INSTRUMENTATION, Vol. 11, No. 1, March 2024 https://doi.org/10.15878/j.instr.202400025

Article

Model Prediction and Optimal Control of Gas Oxygen Content for A Municipal Solid Waste Incineration Process

Aijun Yan[1, 2, 3, *] and Tingting Gu[1, 2]

[1] Faculty of Information Technology, Beijing University of Technology, Beijing 100124, China

[2] Engineering Research Center of Digital Community, Ministry of Education, Beijing 100124, China

[3] Beijing Laboratory for Urban Mass Transit, Beijing 100124, China

[*] Corresponding author email: yanaijun@bjut.edu.cn

Abstract: In the municipal solid waste incineration process, it is difficult to effectively control the gas oxygen content by setting the air flow according to artificial experience. To address this problem, this paper proposes an optimization control method of gas oxygen content based on model predictive control. First, a stochastic configuration network is utilized to establish a prediction model of gas oxygen content. Second, an improved differential evolution algorithm that is based on parameter adaptive and t-distribution strategy is employed to address the set value of air flow. Finally, model predictive control is combined with the event triggering strategy to reduce the amount of computation and the controller's frequent actions. The experimental results show that the optimization control method proposed in this paper obtains a smaller degree of fluctuation in the air flow set value, which can ensure the tracking control performance of the gas oxygen content while reducing the amount of calculation.

Keywords: municipal solid waste incineration; gas oxygen content; stochastic configuration network; model prediction; differential evolution

Citation: Aijun Yan and Tingting Gu. "Model Prediction and Optimal Control of Gas Oxygen Content for a Municipal Solid Waste Incineration Process." *Instrumentation* 11, no. 1 (2024). https://doi.org/10.15878/j.instr.202400025

0 Introduction

With population growth and the acceleration of urbanization in China, the production of municipal solid waste (MSW) is increasing year by year[1]. Presently, the main ways to address MSW are landfilling, composting, and incineration. Compared with landfilling and composting, municipal solid waste incineration (MSWI) with harmlessness, reduction and recycling and other significant advantages and has been a major means to deal with MSW[2]. In the incineration process, the gas oxygen content (GOC) is a key parameter that reflects the incineration efficiency, and if the set value of primary and secondary air flow is unreasonable, it will lead to its unstable control, which will lead to the problem of exceeding the pollutant emission concentration. Therefore, it is important to study how to reasonably set the size of the air flow to ensure the effective control of GOC and the smooth operation of the MSWI process.

Most industrial processes are characterized by nonlinearity, dynamics, time variance, and numerous disturbances. Obtaining the optimal set values of the operating variables to ensure the stable control of the controlled variables remains challenging in the operation optimization of industrial processes. Due to the difficulty of obtaining the mechanism model of industrial processes, and the complex and variable working conditions lead to the accuracy of the mechanism model is difficult to ensure, thus, the mechanism modeling method to obtain the set values of the operating variables has certain limitations[3]. Traditional control methods, such as PID controller, are used to calculate setpoint values that depend on the tuning results of PID parameters, and good control performance cannot be obtained in the face of sudden form changes[4], which will bring uncertain effects to practical applications. Therefore, intelligent optimization setting

methods have gained attention and applications. For example, reference [5] combined case-based reasoning, BP neural networks and other intelligent techniques to set the flotation tank level in the flotation production process. References [6-8] utilized swarm intelligent optimization algorithms to obtain the optimized setting values of operating variables. For the control methods of controlled variables, the quality of the commonly applied PID control significantly decreases in the face of nonlinearity, time variance, strong coupling and uncertainty, while model predictive control (MPC)[9], as a kind of advanced control strategy capable of addressing multivariable and constrained control problems, has a certain degree of adaptivity and robustness, which is extensively used in the areas of autonomous driving[10], power systems[11], and blast furnace ironmaking[12]. The techniques of interest for MPC include the establishment of predictive models and the design of rolling optimization strategies. Due to the advantages of the neural network model in learning data and approximating nonlinear mapping, using it to build prediction model has certain application effects[13, 14]. However, the model needs to consider the problems of falling into a local optimum and slow convergence speeds. The design of the rolling optimization strategy is reflected in the optimization method and optimization efficiency. When using the particle swarm algorithm[15], differential evolution (DE)[16] and other swarm intelligence optimization algorithms, we need to avoid the problem of local optima. In terms of optimization efficiency, we should reduce the number of optimizations to avoid the controller's frequent actions.

Based on the above analysis, an optimal control method of GOC based on MPC is proposed in this paper. The improved differential evolution (IDE) algorithm is applied to the real-time rolling optimization setting of air flow in the MSWI process, and the event triggering strategy is applied to the control system structure to reduce the calculation amount of air flow setting and the frequent update of the controller[17, 18]. The prediction model of GOC is established by using the advantages of a stochastic configuration network (SCN)[19] such as fast convergence speed, and provides an evaluation basis for the IDE optimization algorithm. Through experiments, this method realizes the function of optimal setting of air flow and accurate tracking control of GOC.

The rest of the paper is structured as follows: Section 2 introduces the MSWI process; Section 3 introduces the optimal control methods and implementation steps of GOC. Section 4 presents the experiment and results analysis. Section 5 is a brief summary of our work.

1 MSWI Process

The reciprocating push-type grate furnace of a solid waste incineration plant is selected as an example, and a flow chart of the incineration process is shown in Fig.1. First, domestic waste is mixed with a grab bucket and left to stand in the solid waste storage pool for 3-10 days for fermentation and preliminary drying. Second, the waste is transported via the feeder to the drying grate, where it is further dehydrated and dried by the effect of the primary combustion air and the high temperature of the furnace. Then, the dry MSW is sent to combustion grate 1 and combustion grate 2 for reciprocating movement to achieve combustion and volatiles precipitation. Finally, part of the unburned solid waste is fully burned in the ember grate, and the slag is carried away by the waste carrier.

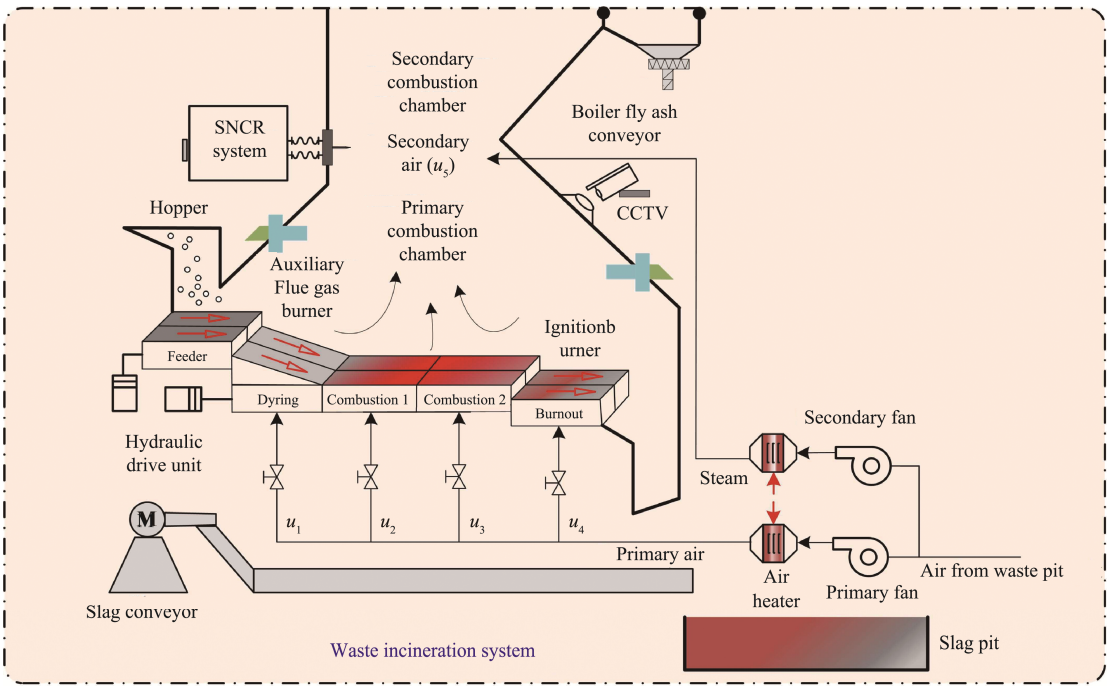

Fig.1 MSWI process flow

As shown in the process flow in Fig.1, the primary air is blown in from below the grate after being heated at a high temperature (there are four sections, namely, the drying section u_1, combustion section u_2, combustion section u_3, and burnout section u_4) to provide oxygen for the whole combustion process. Secondary air u_5 moves from above into the second combustion chamber to promote the further combustion of flue gas and the decomposition of harmful substances. The primary and secondary air flow are two key operating variables in the MSWI process, which directly affect the size of the GOC. When the GOC is low, it will lead to insufficient oxygen in the incinerator to support the solid waste to achieve complete combustion; conversely, it means that the flue gases will carry away more heat, and the heat loss of the exhaust flue becomes larger as a result, and promotes the synthesis of NO*x*. Therefore, it is important to study the setting method of air flow and the control of GOC for the stable combustion of refuse and the complete decomposition of harmful substances. The MSWI process is characterized by nonlinearity, multi-coupling and many interferences, and achieving effective control of GOC is challenging by adjusting the air flow through expert experience, and it is difficult to obtain an accurate process model, which makes it difficult to achieve good performance of the PID controller. As an advanced control strategy, MPC can resolve multivariable and constrained control problems well. It is very important to select the prediction model, improve the accuracy of rolling optimization and decrease the calculation amount of setting for air flow setting and the control of GOC.

2 Optimal Control Method of GOC

To address the subjective and arbitrary nature of manual setting of primary and secondary air flow in the MSWI process and the problem of ineffective control of GOC, an optimal control method of GOC based on model predictive control is proposed. The structure of the method is shown in Fig.2, which mainly includes the reference trajectory, IDE-based rolling optimization, event triggering strategy, SCN prediction model of GOC and feedback correction. The symbols shown are explained as follows: y_{sp} is the set value of the GOC; $y_r(k+j)$ is the reference trajectory; $\hat{y}(k+j)$ is the output value of the j-th step of the GOC prediction model after feedback correction; $U(k)$ is the optimal control law (i.e., the optimized set values of the air flow $u_1 \sim u_5$); $y_p(k)$ is the value of the GOC prediction; and $y_p(k+j)$ is the output value of the j-th step of the GOC prediction model.

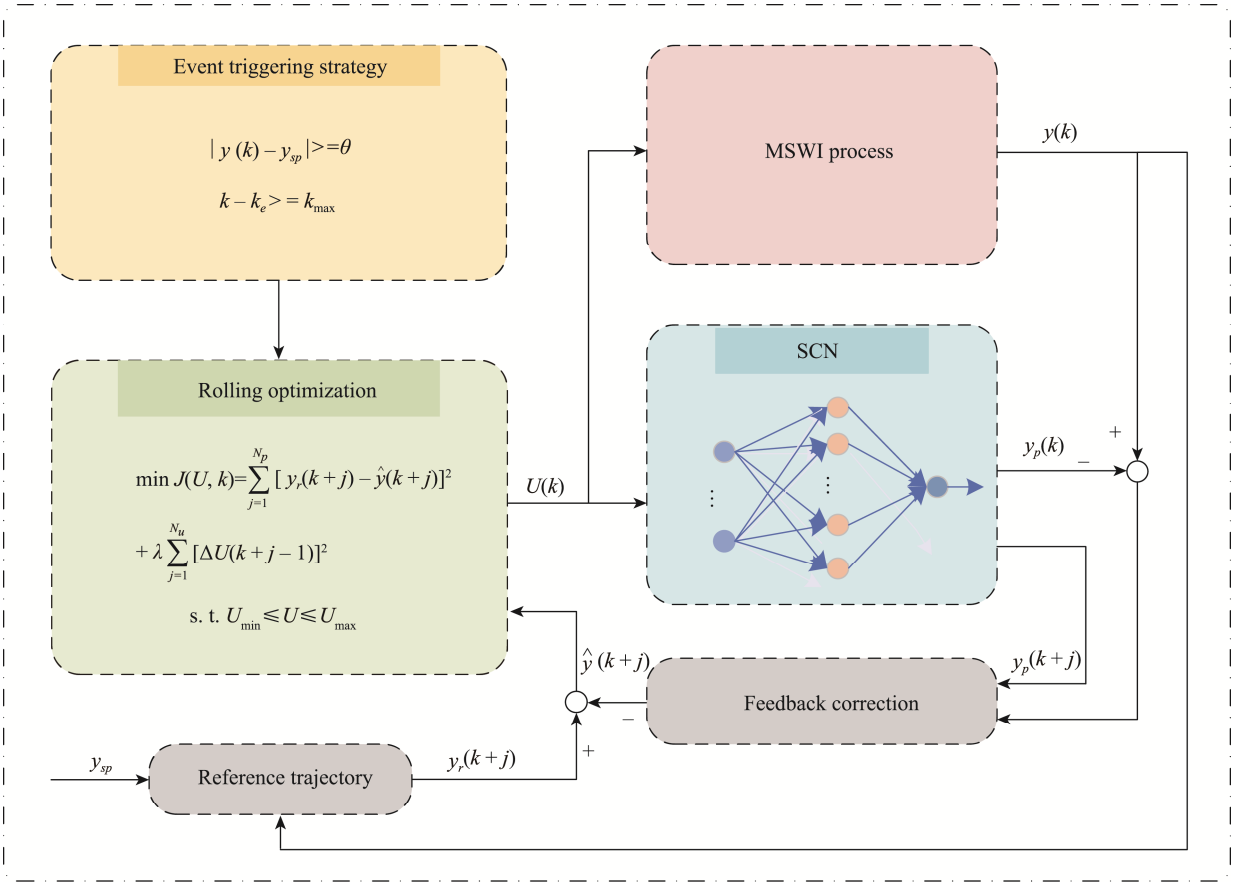

Fig.2 Structure diagram of the set control method for GOC of the MSWI process

2.1 Prediction Model of GOC

The prediction model of GOC is a mathematical description of the relationship between GOC and primary and secondary air flow in the MSWI process and provides an evaluation basis for the optimization algorithm of the air flow set value. The use of the SCN in industrial modeling is widespread due to its high training efficiency and ability to universally approximate nonlinear mapping[20, 21]. Therefore, the SCN network is adopted in this paper to establish a prediction model of GOC, and the output of GOC in the future is predicted according to the set value solved by the rolling optimization strategy and historical GOC information, as shown below:

$$\begin{aligned} y_p(k+1) &= f\left(U(k), y(k)\right) \\ U(k) &= \{u_1(k) \sim u_5(k)\} \end{aligned} \tag{1}$$

where $u_1(k)$-$u_5(k)$ represent the set values of the primary air flow in the drying section, combustion section, combustion section, and embers section and the set value of the secondary air flow.

For the objective function f, the training set of SCN is $\{(U, Y)\}$, assuming that the hidden layer of SCN network has been configured with L-1 nodes, which is described by:

$$f_{L-1}(U;\beta) = \sum_{j=1}^{L-1} \beta_j g_j(\omega_j^{\mathrm{T}} U + b_j) \tag{2}$$

where j = 1, 2,... L-1, w_j and b_j respectively denote the input weight and bias of the j-th hidden layer neuron, β_j denotes the output weight of the j-th hidden layer neuron, and $g_j(\cdot)$ is the activation function of the j-th hidden layer neuron.

Currently, the residuals of the SCN network are defined as:

$$e_{L-1} = f - f_{L-1} \tag{3}$$

If $\|e_{L-1}\|$ does not meet the expected error or the number of nodes in the hidden layer does not meet the expected requirements, a new node needs to be added according to the following formula.

$$\left\langle e_{L-1}, g_L \right\rangle^2 \geq b_g^2 \left(1 - r - \mu_L\right) \left\| e_{L-1} \right\|^2 \tag{4}$$

where $0 < \|g\| < b_g$, $0 < r < 1$. $\{\mu_L\}$ denotes a sequence real numbers, $\lim_{L\to\infty} \mu_L = 0$ and $\mu_L \leq (1 - r)$.

After adding a new node, the output weight is calculated using least square method:

$$\beta^* = \underset{\beta}{\operatorname{argmin}} \left\| G_L \beta - Y \right\|^2 = G_L^{\dagger} Y \tag{5}$$

where β* represents the updated hidden layer output weight matrix, $G_L = \{g_1, g_2, ..., g_L\}$, and $G_L^{\dagger}$ represents the pseudo-inverse of hidden layer output matrix G_L.

2.2 Optimization Solution of the Air Flow Set Value

Model predictive control solves a series of future control actions $U(k)$, $U(k+1)$, …$U(k+N_u)$ by rolling optimization of objective functions, they are not all implemented one by one, only the current control input[22]. The objective function is shown as follows:

$$\begin{aligned} &\min J(U,k) = \sum_{j=1}^{N_p} [y_r(k+j) - \hat{y}(k+j)]^2 + \\ &\lambda \sum_{j=1}^{N_u} [\Delta U(k+j-1)]^2 \\ &\text{s.t. } U_{\min} \leq U \leq U_{\max} \end{aligned} \tag{6}$$

where λ represents the control value coefficient, Np denotes the time domain of prediction, Nu denotes the time domain of control ($N_u \leq N_p$), and $U_{\max}$ and $U_{\min}$ represent the upper and the lower bound of U, respectively.

To smooth the transition of the system output to the set value, the reference trajectory is set up in a first-order smoothing filter:

$$\begin{cases} y_r(k) = y(k) \\ y_r(k+j) = \alpha y_r(k+j-1) + (1-\alpha) y_{sp} \end{cases} \tag{7}$$

where α represents the adjustment factor, $0 < \alpha < 1$.

Because of the effect of system disturbance or model mismatch, there will inevitably be a deviation from the predicted model output to the actual model output. To minimize the discrepancy, feedback compensation uses the difference from the current predicted output to the actual output to ensure that the prediction results are more accurate at the next moment. The specific formula of feedback compensation is as follows:

$$e(k) = y(k) - y_p(k) \tag{8}$$

$$\hat{y}(k+j) = y_p(k+j) + \eta e(k) \tag{9}$$

where $e(k)$ represents the deviation from the predicted model of GOC to the actual output, and η is the compensation coefficient.

Equation (6) is the optimal solution of complex nonlinear constraint problems. The (DE) algorithm has been extensively researched and considered in recent years for its ease of implementation, high search effectiveness, and strong performance in problem-solving [23, 24]. The DE algorithm utilizes the information differences among population individuals to perturb individual information, thereby obtaining excellent progeny individuals, which includes steps such as population initialization, mutation, crossover and selection, specifically described as follows:

Population initialization: The method of randomly initializing the population is generally adopted, and each dimension of the individual is randomly generated according to the following formula.

$$x_{i,j}^0 = x_j^{low} + r \cdot x_j^{up} \tag{10}$$

where i=1, 2, …, NP, j=1, 2,…, D, NP denotes the population size, D denotes the search dimension, $x_{i,j}^0$ is the j-dimensional component of the i-th individual in the 0-th generation, r is the random number between 0 and 1, and x_j^{low} and x_j^{up} represent the minimum value and maximum value, respectively, of an individual on the j-dimension.

Mutation: Mutation generates new individuals by performing a differential operation on each individual within the population. The following DE/current-to-pbest/1 mutation strategy [25] uses the information of multiple optimal solutions, which somewhat balances the greedy nature of mutation and the diversity of the population.

$$v_i^g = x_i^g + F_i \cdot \left(x_{pbest}^g - x_i^g\right) + F_i \cdot \left(x_{r1}^g - x_{r2}^g\right) \quad (11)$$

where g =1, 2, …, G, v_i^g is the mutation vector, and x_i^g is the i-th individual in the g generation population. x_{pbest}^g is the individual randomly selected from the ranking p% excellent individuals of the g generation. F_i represents the mutation factor, and $r1$, $r2$, and i are different integers in the range [1, NP].

Crossover: The aim of the crossover operation is to combine the vector produced by the mutation process with the target individual, resulting in a test individual. The goal is to preserve good features of the parent and to increase the diversity of the population. The binomial crossover method is generally adopted.

$$u_{i,j}^g = \begin{cases} v_{i,j}^g, \ if \ rand(0,1) \le CR_i \ or \ j = j_{rand} \\ x_{i,j}^g, \ otherwise \end{cases} \quad (12)$$

where j_{rand} represents a random number in [1, D] and CR_i represents the crossover probability.

Selection: The fitness values of the test individuals are compared with those of the target individuals, and the individuals with higher fitness are selected as the new generation.

$$x_i^{g+1} = \begin{cases} u_i^g, \ if \ f(u_i^g) < f(x_i^g) \\ x_i^g, \ otherwise \end{cases} \quad (13)$$

Similar to most swarm intelligent optimization algorithms, the DE algorithm also has the problems of easily falling into the local optimum and slow convergence speed. To ensure the quality of solving the set values of the primary and secondary air flow, this paper improves the DE algorithm from the following two aspects: 1) In the mutation strategy, the adaptive t-distribution operator is introduced to outstanding individuals to improve the diversity of the population; 2) The design of the control parameter's adaptive strategy, which uses the evolutionary information of the population to direct the search scope and direction to ensure good convergence performance of the population. The specific implementation process is presented as follows:

1) The adaptive t-distribution operator is introduced to mutate excellent individuals. The DE/current-to-pbest/1 mutation strategy is used to enhance the diversity of the population and avoid local optimality. The adaptive t-distribution operator is introduced to mutate the excellent individual x_{pbest}. The t-distribution is a form of statistical distribution whose curve shape is related to the degree of freedom, and the probability density function is presented below:

$$t(x;\mu,\sigma,v) = \frac{\Gamma((v+1)/2)}{\sqrt{v\pi}\Gamma(v/2)}\left(1+\frac{(x-\mu)^2/\sigma^2}{v}\right)^{-(v+1)/2} \quad (14)$$

where μ and σ represent the position parameter and scale parameter, respectively; v represents the degree of freedom; and $\Gamma(\cdot)$ denotes the gamma function. The smaller the degree of freedom is, the flatter the t-distribution curve is, the lower the middle of the curve is, and the higher the tail on both sides of the curve is. When the degrees of freedom tend to infinity, the t-distribution curve is the standard normal distribution curve. When v is equal to 1, the t distribution is a Cauchy distribution. The comparison plot of the t-distribution with different degrees of freedom is shown in Fig.3:

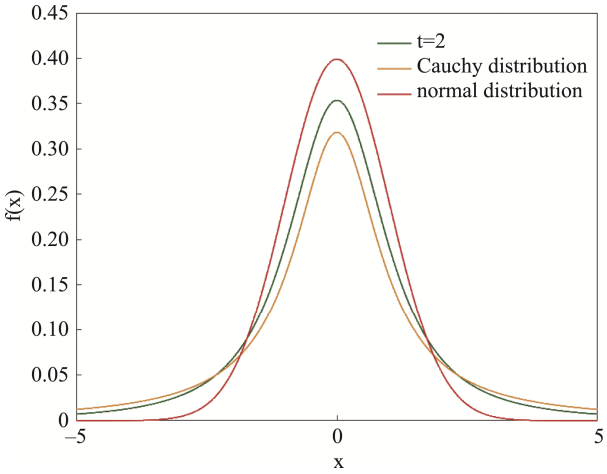

Fig.3 Comparison of T-distributions for different degrees of freedom

The specific implementation of adaptive t-distribution mutation for excellent individuals is expressed as follows:

$$x'_{pbest} = x_{pbest} + x_{pbest} \times trnd(t) \quad (15)$$

where x'_{pbest} represents the position of the excellent individual after x_{pbest} is updated and $trnd(t)$ represents the t-distribution function whose degree of freedom is t (that is, the number of current iterations). In the early phase of evolution, the algorithm can overcome the problem of premature convergence because the degree of freedom of the t-distribution is small and the perturbation of excellent individuals is large. In the later phase of evolution, as the value of the degrees of freedom increases, the influence of the t-distribution mutation decreases, which enables the algorithm to perform a better search in the local scope and accelerate the convergence speed. When the fitness value of the excellent individual after mutation is less than that of the original excellent individual, the mutated individual will replace the excellent individual to continue the mutation of the target individual; otherwise, the excellent individual will remain unchanged. The selection method of the excellent individual x_{pbest} is shown in the following equation:

$$x_{pbest} = \begin{cases} x'_{pbest}, \ if \ (x'_{pbest}) < f(x_{pbest}) \\ x_{pbest}, \ else \end{cases} \quad (16)$$

2) Adaptive adjustment of control parameters. The F and CR directly affect the search scope and direction of the next generation, and the fixed parameter method

cannot meet the requirements well. In this paper, the evolutionary information of the population is used to adaptively adjust the control parameters to improve the optimization performance of the algorithm. The improved algorithm will retain the control parameters that produce excellent individuals and regenerate the parameters that produce obsolete individuals using a normal distribution, as shown below:

$$F_i = \begin{cases} randc_i\left(\mu_F, 0.1\right), \ if \ \ (u_i^g) < f(x_i^g) \\ F_i, \ else \end{cases} \tag{17}$$

$$CR_i = \begin{cases} randc_i\left(\mu_{CR}, 0.1\right), \ if \ \ (u_i^g) < f(x_i^g) \\ CR_i, \ else \end{cases} \tag{18}$$

where the average values μ_F and μ_{CR} are initialized to 0.5 and both are updated in the same way. Selecting μ_F as an example, it is specifically updated according to the following equation:

$$\mu_F = (1-c)\cdot \mu_F + c \cdot mean_L\left(S_F\right) \tag{19}$$

where c is a number between [0, 1], S_F represents the successful mutation factors per generation, and $\text{mean}_L(.)$ is calculated using the Lehmer mean as follows:

$$mean_L\left(S_F\right) = \frac{\sum\limits_{F\in S_F} F^2}{\sum\limits_{F\in S_F} F} \tag{20}$$

In summary, by introducing the adaptive t-distribution operator into the DE mutation strategy to increase the diversity of the population, the adaptive strategy of the control parameters is designed, and the evolutionary information of the population is used to guide the search range and direction and obtain the IDE. The algorithm's pseudocode is shown below:

Algorithm 1: IDE pseudocode

Input: population size *NP*, maximum number of iterations *G*, search dimension *D*, and search interval [*lb*, *ub*].

Output: Optimal set value of the solved primary and secondary air flow.

```
Initialize the population according to Eq. (10);
Calculate the fitness value of the initial population according to Eq. (6);
for g = 1: G
    S_F=Ø, S_CR= Ø;
    for n = 1: NP
        Randomly select excellent individuals x_pbest, and randomly select the individuals x_r1^g and x_r2^g;
        Mutate the t-distribution of superior individuals according to Eq. (15), and select the superior
        individuals according to Eq. (16);
        Mutate the individuals according to Eq. (11);
        Cross the individuals according to Eq. (12);
        Select the operation according to Eq. (13);
        Calculate the mutation factor and crossover probability of the i-th individual of the next generation
        according to Eq. (17) and Eq. (18);
    end for
        Recalculate the mean values of the mutation factor and crossover probability according to Eq. (19)
        and Eq. (20);
end for
```

2.3 Event Triggering Mechanism Design

In a typical MPC algorithm, at each time step, the optimal solution to the finite-time control problem must be searched repeatedly, which consumes considerable computing resources [26]. To solve the problem of calculating the high frequency, this paper introduces an event trigger strategy. Only when the system meets the trigger conditions will the value of the controller be updated (i.e., for the primary and secondary air flow setting calculation). Two trigger conditions are designed here. When one of the following conditions is met, the resetting of the air flow is triggered.

(1) Fixed threshold trigger design

$$\left|y_{sp}(k) - y(k)\right| \geq \theta \tag{21}$$

If the absolute error between the set value of the GOC and the actual output reaches a threshold value θ, a new event is triggered.

(2) Fixed event trigger design

$$k - k_e \geq k_{\max} \tag{22}$$

where k_e is the last triggered moment and $k_{\max}$ is the maximum allowable time limit. If the maximum allowed time limit is reached since the last trigger, a new event is triggered.

Based on the above, first, the SCN prediction model of the GOC is established, and the IDE algorithm is employed to solve the rolling optimization of MPC. The event-triggered is combined with MPC to reduce the calculation of the optimization setting and the number of controller updates. The flow chart of the GOC optimization control method is shown in Fig.4:

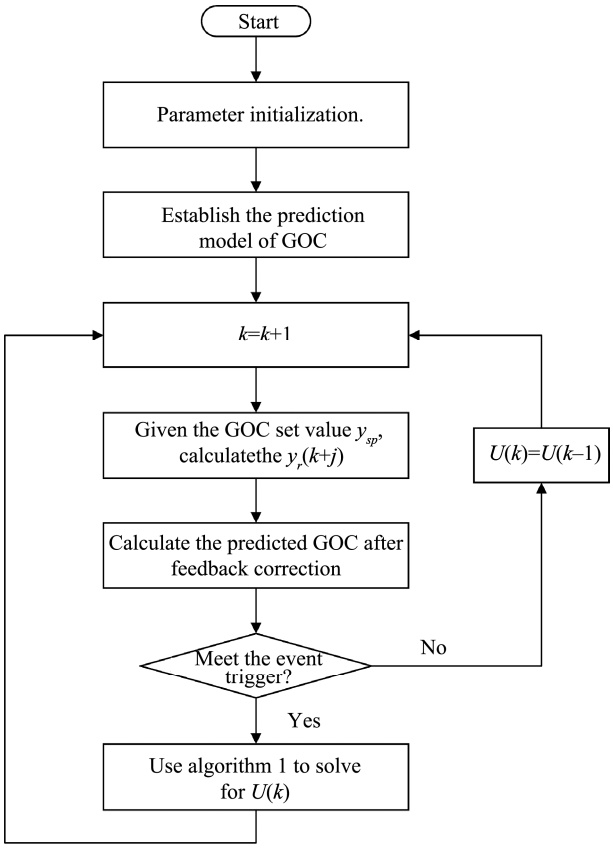

Fig.4 The Flow chart of the GOC optimization control method

3 Experiments and Analysis of Results

To realize the optimized setting of the air flow of the MSWI process and the stable control of the GOC, this paper proposes an optimized control method of the GOC based on model predictive control. The effectiveness of the proposed method is verified by three experiments. The first is a comparison experiment of different GOC prediction models. The second tests the optimization ability of IDE as a rolling optimization strategy. In the third experiment, the effectiveness of the overall optimization and control method is verified.

3.1 Comparison of Prediction Models of GOC

To test the accuracy of the GOC model, the SCN is compared with BP and the random functional-link network (RVFL) [27], which are classical modeling methods for experiments. There are 1000 real data collected from the on-site DCS system of the solid waste incineration plant utilized for testing, and the sampling period is 10 s. The number of training samples is 800, the number of test samples is 200, all the data are normalized. The prediction results of the above methods are compared using three different evaluation indexes: mean absolute percentage error (MAPE), root mean square error (RMSE), and determination coefficient (R^2). The formulas are shown below:

$$\mathrm{MAPE}=\frac{1}{N}\sum_{n=1}^{N}\frac{\left|y_d(n)-y_p(n)\right|}{y_d(n)}\times 100\% \tag{23}$$

$$\mathrm{RMSE}=\sqrt{\frac{1}{N}\sum_{n=1}^{N}(y_d(n)-y_p(n))^2} \tag{24}$$

$$\mathrm{R}^2=1-\frac{\sum_{n=1}^{N}(y_d(n)-y_p(n))^2}{\sum_{n=1}^{N}(y_d(n)-\overline{y_p}(n))^2} \tag{25}$$

where N is the number of samples, y_d is the real value and y_p is the predicted value.

The parameters of the experimental process are set as follows: the maximum hidden layer nodes of the SCN is 10, the maximum number of configurations is 100, the expected training error is set to 0.001, and the activation function is chosen as the Sigmoid function In the RVFL model, the parameters are kept the same as those of SCN. In the BP model, the learning rate is 0.01, the number of training times is 100, and the rest of the settings are kept the same as those of SCN.

Table 1 lists the mean values of the results of 20 independent experiments for different models (the bold font in the table indicates the optimal values). The SCN prediction model's MAPE, RMSE and R^2 are 0.0625, 0.0283 and 0.9489, respectively, which are superior to BP and RVFL. Fig.5 shows the prediction results of the BP, RVFL, and SCN networks for GOC, which shows that the SCN has the highest prediction performance for GOC. The main reason for the above results is that the SCN network avoids the gradient descent method of the BP algorithm, which easily falls into the problem of local optima. Compared with the RVFL network, the SCN can better approximate the actual output due to the addition of the inequality supervisory mechanism, which lays a foundation for the optimization of the air flow setting of the MSWI process and the control of GOC.

Table 1 Comparison of evaluation indexes for GOC prediction by different modeling methods

Model	MAPE	RMSE	R^2
BP	0.0695	0.0322	0.9351
RVFL	0.0690	0.0315	0.9348
SCN	**0.0625**	**0.0283**	**0.9489**

3.2 Comparison of IDE Optimization Ability

To verify the effectiveness of the IDE algorithm using parameter adaptive and t-distribution based strategies in this paper, the improved differential evolutionary algorithm using only parameter adaptive is denoted as IDE1, and the setup control effects of DE, IDE1 and IDE as rolling optimization strategies are compared. The experimental parameters are set as follows: the SCN model parameters are kept consistent with the

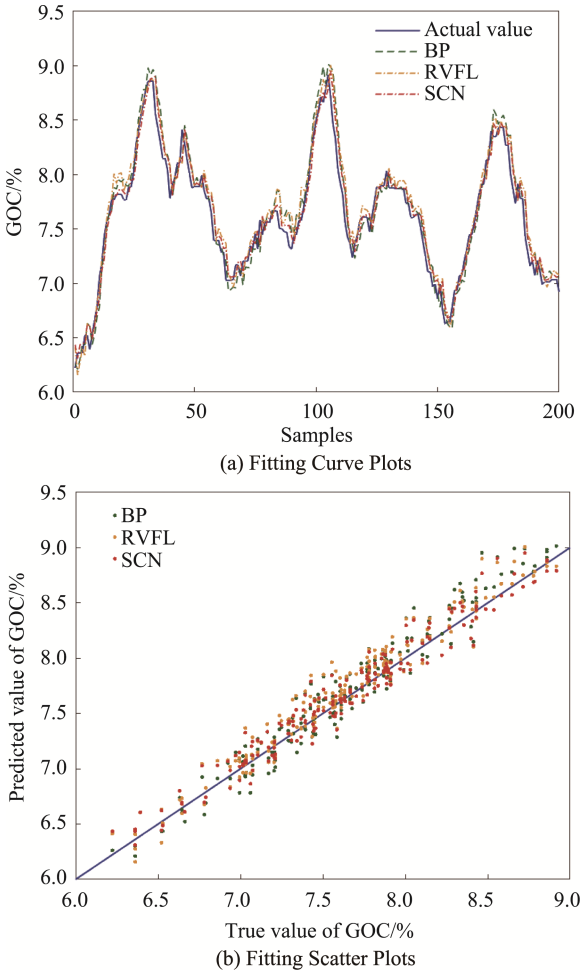

Fig.5 Comparison of the prediction effect of different GOC models

previous section. In DE, IDE1, and IDE, the number of populations is 50, and the maximum number of iterations is 100. The mutation factor F and the crossover factor CR in DE are kept consistent with those in [25], which are 0.5 and 0.9, respectively. The prediction time domain N_p is 3 and the control time domain N_u is 2. The softening coefficient α is 0.2, the compensation coefficient η is 0.3, and the control weighting coefficient λ is 0.1. In addition, the range of variation of the input and output variables in the historical data is shown in the following table:

The tracking control performance of different GOC setpoints when DE, IDE1 and IDE are utilized as rolling optimization strategies is shown in Fig.6. It can be seen that the DE algorithm using parameter adaptive improvement retains the parameters that produce quality solutions and improves the convergence speed, so IDE1 is better than DE when it is used as a rolling optimization strategy. IDE increases the adaptive t-distribution operator to mutate the excellent individuals and enhance the diversity of the population relative to IDE1. Therefore, IDE is more effective when it is used as a rolling optimization strategy, and can achieve more accurate and fast tracking of GOC, which verifies the effectiveness of the two improvement methods proposed in this paper to improve the optimization ability of the DE algorithm.

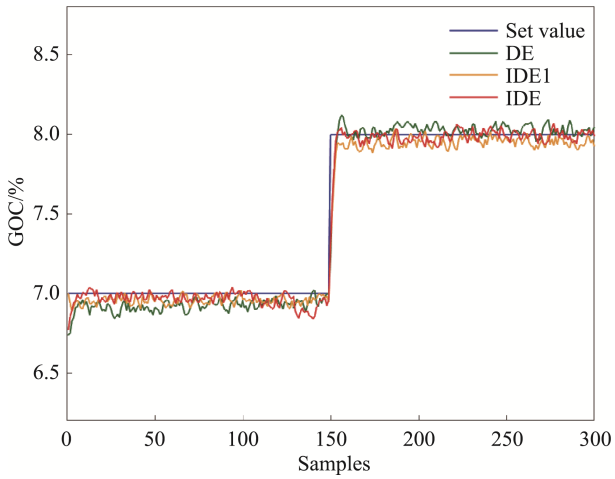

Fig.6 Tracking curves of GOC setpoints with different rolling optimization strategies

To further verify the optimization ability of the IDE algorithms, Table 3 compares the control results of the above optimization methods by three different evaluation indexes, including the integral of squared error (ISE), integral absolute error (IAE) and maximal deviation from setpoint ($\mathrm{Dev}^{\max}$), which are shown in the following formula:

$$\mathrm{ISE}=\sum_{t=1}^{k}{e_{OC}}^{2} \tag{26}$$

$$\mathrm{IAE}=\sum_{n=1}^{N}\left|e_{OC}(k)\right| \tag{27}$$

$$\mathrm{Dev}^{\max}=\max\left\{\left|e_{OC}\right|\right\} \tag{28}$$

where N represents the total number of samples and e_{oc} represents the error between the set value of GOC and true value of GOC.

As can be seen from Table 3, when IDE1 is used as the rolling optimization strategy, ISE, IAE and $\mathrm{Dev}^{\max}$ are 1.7173, 15.4282 and 0.7141, respectively, which is better than DE strategy. The evaluation indexes of IDE are the best, which were reduced by 18.64%, 23.11% and 2.69% compared with IDE1 strategy and 39.18%, 35.54% and 11.05% compared with DE strategy, respectively. It shows the effectiveness of the improved DE algorithm proposed in this paper.

In addition, when IDE is utilized as a rolling optimization strategy, the setting process of primary and secondary air flows is shown in Fig.7, which reduces the maximum deviation of air flow fluctuation by 81.76%, 81.72%, 69.71%, 53.46%, and 56.89% compared to that of the manual setting method, with a smaller fluctuation range, which is conducive to the stability of the system.

3.3 Event Trigger Setting Results

To verify the effectiveness of the event-triggered strategy designed in this paper, the setup control method with a triggering mechanism (briefly referred to as ET-IDE) is compared with one-step-ahead predictive control (OSPC) and IDE as a rolling optimization control

Table 2 Range of variation of input and output variables

Name	Variable symbol	Range of variation
Primary air flow in the drying section	u_1	14.68 ~ 21.32 km^{3}N/h
Primary air flow in the first section of combustion	u_2	7.41 ~ 13.82 km^{3}N/h
Primary air flow in the second section of combustion	u_3	17.62 ~ 29.53 km^{3}N/h
Primary air flow in the burnout section	u_4	4.25 ~ 14.84 km^{3}N/h
Secondary air flow	u_5	1.41 ~ 50.16 km^{3}N/h
GOC	y	5.81% ~ 10.24%

Table 3 Tracking evaluation of GOC setpoints with different rolling optimization strategies

Evaluation indexes	ISE	IAE	Dev^{max}
DE	2.2973	18.4032	0.7812
IDE1	1.7173	15.4282	0.7141
IDE	**1.3972**	**11.8625**	**0.6949**

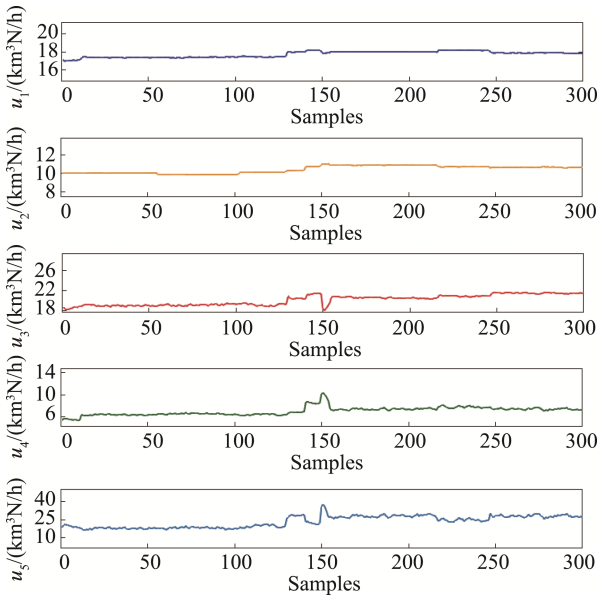

Fig.7 Primary and secondary air flow setting curves when IDE is employed as a rolling optimization strategy

method. It should be pointed out that the OSPC here is obtained by taking both the prediction time domain N_p and the control time domain N_u in the MPC control as 1. The error triggering threshold θ set to 0.05, the maximum allowable time limit k_{max} set to 10, and other experimental parameters consistent with those in the previous section. The tracking performance of the three control methods for different GOC setpoints is shown in Fig.8, which shows that compared with the OSPC control, the IDE and ET-IDE methods utilize the multi-step prediction information of the GOC prediction model to solve the optimal control law, and they can adapt to the slow time-varying and large hysteresis characteristics of the GOC changes, and can follow the GOC setpoints quickly and smoothly. To further show the performance of the ET-IDE method, the comparison results of the three evaluation indexes and the number of events are given in Table 4. It can be seen that the ISE, IAE and Dev^{max} of the ET-IDE method are better than the performance indexes of the OSPC method, and the control effect of IDE as a rolling optimization strategy is close to that of IDE, but the number of triggering events is much less than that of the traditional MPC method. Its air flow setting curve is shown in Fig.9, with a small fluctuation range, which is conducive to the stable control of GOC.

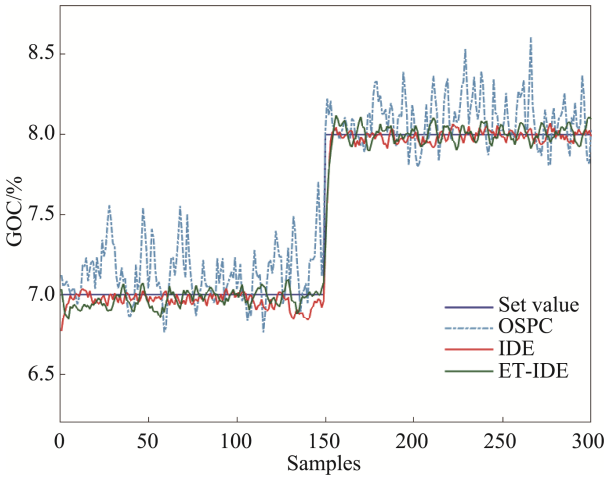

Fig.8 Tracking curves of GOC setpoints for different control methods

Table 4 Tracking evaluation of GOC setpoints with different control methods

Evaluation indexes	ISE	IAE	Dev^{max}	Number of events
OSPC	11.6435	45.2332	0.7033	300
IDE	**1.3972**	**11.8625**	**0.6949**	300
ET-IDE	1.6289	14.6870	0.7135	**140**

The event-triggering interval diagram of the method proposed in this work is shown in Fig.10. The traditional MPC method needs to set the calculation and update the controller 300 times, while the method proposed in this paper only needs to update the controller 140 times. In summary, the experimental results show that the event-triggered setting method effectively reduces the calculation burden and the frequent action of the controller under the premise of satisfying the control accuracy.

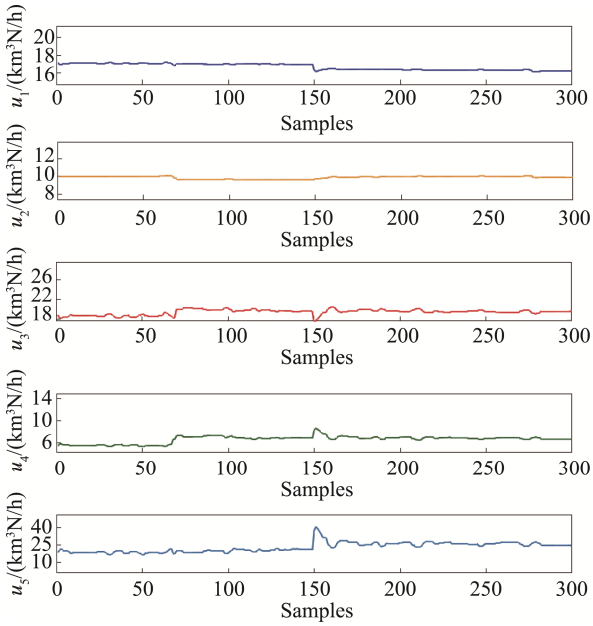

Fig.9 Primary and secondary air flow setting curves for the ET-IDE method

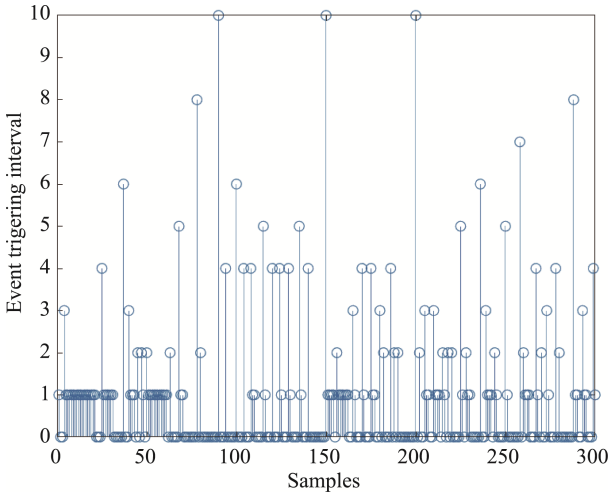

Fig.10 Event triggering interval for ET-IDE methods

4 Conclusion

To realize the optimal setting of the primary and secondary air flows of the MSWI process and the stable control of the GOC, this paper proposes an optimization control method based on MPC, establishes a GOC prediction model based on the SCN, implements a rolling optimization algorithm based on IDE, designs an event-triggered strategy for solving the setting values of the air flow, and employs operation data of the MSWI process to verify the effectiveness of this optimization control method. The main contributions of the methodology in this paper are summarized as follows:

First, the GOC prediction model established by the SCN can avoid the problem that the gradient descent method easily falls into the local optima, and the prediction accuracy is high, which lays a foundation for the optimized setting of primary and secondary air flow and the stable control of GOC.

Second, the improved DE algorithm using parameter adaptive and t-distribution strategy can improve the solution performance of rolling optimization. Compared with the manual setting method, the fluctuation range of air flow is smaller, which is conducive to the stable operation of the control system.

Third, the designed event triggering strategy can effectively reduce the calculation amount of air flows solution under the premise of satisfying the control range of GOC and avoid the loss of execution equipment caused by frequent controller action.

The experimental results show that the method proposed in this paper can realize the optimization of the setting of the air flow, avoiding the subjectivity of manual setting based on experience and realizing the accurate control of the GOC. In addition, the designed event triggering mechanism can reduce the amount of setup calculations under the premise of guaranteeing accuracy, which is conducive to improving the efficiency of online control. For the stable control of GOC, in addition to the optimizing the set value of the air flow, solid waste feeding volume, furnace temperature and other parameters of the change will also affect GOC. How to proceed from the analysis of these influencing factors for the change law of the mechanism, by comprehensively considering their control of GOC to realize the multivariate, multi-objective optimization control is the focus of subsequent attention.

Author Contributions:

Contributions：YAN Aijun: Project administration , Supervision, Writing - review & editing. GU Tinting: Writing - original draft and Writing - review & editing.

Funding Information:

This work is supported by the National Natural Science Foundation of China (62373017, 62073006) and the Beijing Natural Science Foundation of China (4212032).

Data Availability:

The data that support the results of this study are available upon reasonable request by contacting the corresponding author.

Conflict of Interest:

The authors declare no competing interests.

Dates:

Received 9 December 2023; Accepted 1 March 2024; Published online 31 March 2024

References

[1] Nanda S, Berruti F (2021). Municipal solid waste management and landfilling technologies: a review. *Environmental Chemistry Letters*, 19(2), pp. 1433-1456.

[2] Xue Y, Liu X (2021). Detoxification, solidification and recycling of municipal solid waste incineration fly ash: A review. *Chemical Engineering Journal*, 420(5), pp. 130349.

[3] Chai T Y (2013). Operational optimization and feedback control for complex industrial processes. *Acta Automatica Sinica*, 39(11), pp. 1744-1757.

[4] Shi K J, Li B, Wang F M, et al (2019). Research on the RBF-PID control method for the motor actuator used in a UHV GIS disconnector. *The Journal of Engineering*, 2019(16), pp. 2013-2017.

[5] Zhao H W, Xie Y F, Jiang Z H, Xu D G, Yang C H, Gui W H (2014). An intelligent optimal setting approach based on froth features for level of flotation cells. *Acta Automatica Sinica*, 40(6), pp. 1086-1097.

[6] Wang C, Yang L, Song Z, Jiang A (2018). Optimizing combustion of coal fired boilers for reducing NOx emission using Gaussian Process. *Energy*, 153(6), pp. 149-158.

[7] Zhou P, Song H D, Wang H, Chai T Y (2016). Data-driven nonlinear subspace modeling for prediction and control of molten iron quality indices in blast furnace ironmaking. *IEEE Transactions on Control Systems Technology*, 25(5), pp. 1761-1774.

[8] Cui Y Y, Meng X, Qiao J F (2023). The intelligent optimization setting method of air flow for municipal solid wastes incineration process. *Control and Decision*, 38(2), pp. 318-326.

[9] Gao T Y, Luo H, Yin S, Kaynak O (2020). A recursive modified partial least square aided data-driven predictive control with application to continuous stirred tank heater. *Journal of Process Control*, 89(5), pp. 108-118.

[10] Wang H Y, Liu B, Ping X Y, An A Q (2019). Path Tracking Control for Autonomous Vehicles Based on an Improved MPC. *IEEE Access*, 7(10), pp. 161064-161073.

[11] Karamanakos P, Liegmann E, Geyer T, Kennel, R, (2020). Model Predictive Control of Power Electronic Systems: Methods, Results, and Challenges. *IEEE Open Journal of Industry Applications*, 1(8), pp. 95-114.

[12] Zhou P, Dai P, Song H, Chai T Y (2017). Data-driven recursive subspace identification based online modelling for prediction and control of molten iron quality in blast furnace ironmaking. *IET Control Theory & Applications*, 11(14), pp. 2343-2351.

[13] Jia R, Zhang S L, You F Q (2021). Nonlinear soft sensor development for industrial thickeners using domain transfer functional-link neural network. *Control Engineering Practice*, 133(8), pp. 1-14.

[14] Lopez-Garcia T B, Coronado-Mendoza A, Domínguez-Navarro J A (2020). Artificial neural networks in microgrids: A review. *Engineering Applications of Artificial Intelligence*, 95(9), pp. 1-14

[15] Kennedy J, Eberhart R C (1995). Particle swarm optimization. *In Proceedings of the IEEE International Conference on Neural Networks*, pp. 1942-1948.

[16] Storn R, Price K (1997). Differential evolution–a simple and efficient heuristic for global optimization over continuous spaces. *Journal of global optimization*, 11(4), pp. 341-359.

[17] Boruah N, and B K Roy (2019). Event triggered nonlinear model predictive control for a wastewater treatment plant. *Journal of Water Process Engineering*, 32(12), pp. 100887.

[18] Feng Z X, Li Y G, Sun B, Yang C H, Zhu H Q, Chen Z S (2021). A trend-based event-triggering fuzzy controller for the stabilizing control of a large-scale zinc roaster. *Journal of Process Control*, 97(12), pp. 59-71.

[19] Wang D H, Li M (2017). Stochastic configuration networks: fundamentals and algorithms. *IEEE Transactions on Cybernetics*, 47(10), pp. 3346-3479.

[20] Dai W, Li D P, Zhou P, Chai T Y (2019). Stochastic configuration networks with block increments for data modeling in process industries. *Information Sciences*, 484(5), pp. 367-386.

[21] Li X, He Y D, Ding J G, Luan F, Zhang D H (2022). Predicting hot-strip finish rolling thickness using stochastic configuration networks. *Information Sciences*, 611(9), pp. 677-689.

[22] Mayne D Q (2014). Model predictive control: Recent developments and future promise. *Automatica*, 50(12), pp. 2967-2986.

[23] Qiao J F, Hou Y, Han H G (2019). Optimal control for wastewater treatment process based on an adaptive multi-objective differential evolution algorithm. *Neural Computing & Applications*, 31(7), pp. 2537-2550.

[24] Li S J, Gu Q, Gong W Y, Ning B (2020). An enhanced adaptive differential evolution algorithm for parameter extraction of photovoltaic models. *Energy Conversion and Management*, 205(2), pp. 112443.

[25] Zhang J, Sanderson A C (2009). JADE: Adaptive Differential Evolution with Optional External Archive. *IEEE Transactions on Evolutionary Computation*, 13(5), pp. 945-958.

[26] Hadian M, Mehrshadian M, Karami M, Biglary Makvand A (2021). Event-based neural network predictive controller application for a distillation column. *Asian Journal of Control*, 23(2), pp. 811-823.

[27] Pao Y H, Park G H, Sobajic D J (1994). Learning and generalization characteristics of random vector functional-link net. *Neurocomputing*, 6(2), pp. 163-180.